

## Witnessing environment induced topological phase transitions via quantum Monte Carlo and cluster perturbation theory studies

F. Pavan,<sup>1</sup> A. de Candia,<sup>2,3</sup> G. Di Bello,<sup>1</sup> V. Cataudella,<sup>2,3</sup> N. Nagaosa,<sup>4</sup> C. A. Perroni,<sup>2,3</sup> and G. De Filippis<sup>2,3</sup>

<sup>1</sup>*Dip. di Fisica E. Pancini - Università di Napoli Federico II - I-80126 Napoli, Italy*

<sup>2</sup>*SPIN-CNR and Dip. di Fisica E. Pancini - Università di Napoli Federico II - I-80126 Napoli, Italy*

<sup>3</sup>*INFN, Sezione di Napoli - Complesso Universitario di Monte S. Angelo - I-80126 Napoli, Italy*

<sup>4</sup>*RIKEN Center for Emergent Matter Science (CEMS), Wako, Saitama 351-0198, Japan*



(Received 8 September 2023; revised 27 December 2023; accepted 23 February 2024; published 21 March 2024)

Many-body interactions play a crucial role in quantum topological systems, being able to impact or alter the topological classifications of noninteracting fermion systems. In open quantum systems, where interactions with the environment cause dissipation and decoherence of the fermionic dynamics, the absence of Hermiticity in the subsystem Hamiltonian drastically reduces the stability of the topological phases of the corresponding closed systems. Here we investigate the nonperturbative effects induced by the environment on the prototype Su-Schrieffer-Heeger chain coupled to local harmonic oscillator baths through either intracell or intercell transfer integrals. Despite the common view, this type of coupling, if suitably engineered, can even induce a transition to topological phases. By using a world-line quantum Monte Carlo technique we determine the phase diagram of the model proving that the bimodality of the probability distribution of the polarization signals the emergence of the topological phase. We show that a qualitative description can be obtained by using an approach based on the cluster perturbation theory providing, in particular, a non-Hermitian Hamiltonian for the fermionic subsystem and insights on the dissipative dynamics. We prove that non-Hermitian effects disappear in the presence of classical heat baths.

DOI: [10.1103/PhysRevB.109.115147](https://doi.org/10.1103/PhysRevB.109.115147)

### I. INTRODUCTION

Topological condensed matter physics is a relatively new field of research that has garnered significant interest in recent years [1–8]. Topological properties can give rise to new states of matter that are protected from external disturbances, exhibiting unique and nontrivial characteristics. Robustness of these states represents a very peculiar feature, fundamental in the context of quantum technologies, from quantum information and quantum computing [9–12] to ultracold atoms [13–21] and topological photonics [22–25].

Commonly phase transitions are classified according to their critical behavior within the framework of Landau-Ginzburg-Wilson theory [26]. It includes concepts like scaling laws and critical exponents, typically associated with local order parameters undergoing a continuous or discontinuous change. Topological phase transitions, on the other hand, do not fit within this framework. They can manifest as the appearance or disappearance of gapless edge or surface states, or the modification of topological invariants, described by global properties, such as the Chern number. Internal symmetries (time-reversal, particle-hole, and chiral symmetries) of the bulk Hamiltonian play a central role in the theory and all possible combinations thereof give rise to the Altland-Zirnbauer classification [27].

The natural question addressed in the last decade is if interactions can influence the topological phases of matter and alter the classifications of noninteracting fermion systems. It has been proved that these influences can manifest in diverse

manners. Interactions between particles can destroy topological phases, but, in some cases, can even induce novel topological phases that are not possible in noninteracting systems [28]. This opens the possibility to take advantage from interactions between the particles to tune between different topological phases [29–31].

There is another way to affect the topological properties: it stems from the interaction between two different fields. A typical example is provided by open quantum systems [32,33]. Since perfect isolation of quantum systems is impossible, interaction with the environment plays a crucial role: it can affect the system even in a nonperturbative way [34–37]. The environment is usually described by an infinite set of quantum harmonic oscillators whose frequencies and coupling strengths obey specific distributions. Then the interaction of the system particles with the environment is concerned with the physics of two coupled fields. Exact elimination of the environment degrees of freedom leads to a time retarded effective interaction and a non-Hermitian Hamiltonian (NHH) for the system under consideration, inducing dissipation, loss of coherence and information. At first glance it is expected to be detrimental to preserve topological phases of matter. In this framework, the search of a theory capable of generalizing topological phase transitions for physical systems described by NHH has been the focus of an extensive research activity [38–42]. Most studies of the last decade concerned with the investigation of NHHs describing noninteracting particles in the presence of *ad hoc* terms simulating the presence of the environment. The spectrum turns out to be complex and the

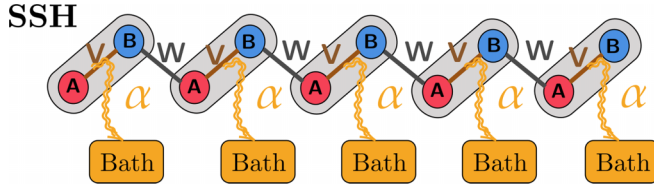


FIG. 1. Schematic view of the SSH model in the presence of intracell hopping coupled with local bosonic baths.

time evolution is not unitary. In other cases the environment is taken into account through Lindblad master equation approach that is appropriate in the limit of weak Markovian interaction [43].

In order to go beyond these approximations, we include the environment in the Hamiltonian that describes the simplest one-dimensional model exhibiting topological features, i.e., the Su-Schrieffer-Heeger (SSH) model: spinless fermions on a lattice with a two site unit cell at half-filling. Electrons are coupled with local bosonic baths in two different ways, i.e., modulating either intracell hoppings  $v$  or intercell hopping  $w$ . Note that in our description, where the quantum bath dynamics is explicitly taken into account, the full Hamiltonian is Hermitian. Since, in general, decoherence effect is viewed as an undesirable destructing factor, the main question we want to address is: Can the coupling with the environment be tailored such that topology is induced in a trivial insulator? By using a quantum Monte Carlo (QMC) approach, we prove that, in one of the two investigated cases, fermion-boson interaction turns a trivial phase in a topological insulating phase. Furthermore we show that, if open boundary conditions are adopted, the polarization distribution displays a bimodal character near the topological phase transition, both in the absence and in the presence of interaction with the environment, signaling the appearance of edge states. This approach is capable to unveil the emergence of topological quantum phase transitions. Finally we propose a simple description of the static and dynamical properties of the fermionic system by using cluster perturbation theory (CPT) [44,45] and periodic boundary conditions in the thermodynamic limit. We derive also an effective NHH for electrons, pointing out the validity of bulk-boundary correspondence in the considered models.

## II. THE MODEL

The SSH model [46,47] (see Fig. 1) describes spinless fermion hopping on a 1D chain with staggered hoppings. The chain is made up by  $N$  unit cells, everyone containing two sites, indicated with the sublattice indices  $A, B$ . The Hamiltonian is the sum of two contributions  $H_{\text{SSH}} = H_v + H_w$ ,

$$H_{\text{SSH}} = \left( v \sum_{n=1}^N c_{n,A}^\dagger c_{n,B} + w \sum_{n=1}^{N-1} c_{n+1,A}^\dagger c_{n,B} \right) + \text{H.c.} \quad (1)$$

Here  $c_{n,v}$  ( $c_{n,v}^\dagger$ ) destroys (creates) an electron in the site  $v = A, B$  of the  $n$ th cell, with  $n = 1, \dots, N$ , and  $v$  ( $w$ ) denotes the intra(inter)cell hopping. This simple toy model underlines the main physical features of topological insulators at half filling. When open boundary conditions are adopted, the

trivial insulating phase is obtained for  $v > w$ , whereas the topological phase, characterized by the appearance of gapless edge states, sets in at  $v < w$ . On the other hand, in the thermodynamic limit and assuming periodic boundary conditions, the presence of spontaneous polarization is marked by a topological invariant  $\eta$  that assumes a nonvanishing value in a discontinuous way. Here we investigate the SSH chain in the presence of local heat baths,  $H = H_{\text{SSH}} + H_B + H_{\text{SSH}-B}$ .  $H_B = \sum_n H_{B,n}$  describes the environment, i.e., local baths where each of them is a collection of harmonic oscillators with frequencies  $\omega_{\alpha,n}$ ,  $H_{B,n} = \sum_\alpha \omega_{\alpha,n} b_{\alpha,n}^\dagger b_{\alpha,n}$ , and  $H_{\text{SSH}-B}$  denotes the fermion-boson interaction,

$$H_{\text{SSH}-B} = \sum_{\alpha,n} g_{\alpha,n} (b_{\alpha,n}^\dagger + b_{\alpha,n}) H_{\text{hop},n}. \quad (2)$$

In Eq. (2)  $H_{\text{hop},n}$  describes the intra- ( $c_{n,A}^\dagger c_{n,B} + \text{H.c.}$ ) or the intercell ( $c_{n+1,A}^\dagger c_{n,B} + \text{H.c.}$ ) fermionic hopping. We limit our attention to Ohmic baths, i.e., the spectral density is given by  $J(\omega) = \sum_\alpha g_{\alpha,n}^2 \delta(\omega - \omega_{\alpha,n}) = \alpha \tilde{\omega} (\frac{\omega}{\omega_D}) e^{-\omega/\omega_D}$  independently on  $n$ . Here the adimensional parameter  $\alpha$  measures the strength of the coupling,  $\omega_D$ , Debye frequency, denotes the cutoff frequency, the largest energy scale, and  $\tilde{\omega}$  is equal to  $v$  ( $w$ ) for intra(inter)cell couplings between fermions and bosons. In the following we fix  $\omega_D = 10w$  and use units such that  $\hbar = a = e = k_B = 1$ ,  $a$ ,  $e$  and  $k_B$  being the lattice parameter, electronic charge and Boltzmann constant, respectively. We emphasize that the Hamiltonians considered in this letter fulfill both particle-hole and chiral symmetries, i.e., the symmetries of the bare SSH model are not broken.

## III. OPEN BOUNDARY CONDITIONS: QMC APPROACH

### A. QMC algorithm

The concept of macroscopic polarization is crucial for describing dielectric media. Polarization operator represents the dipole electrical momentum per unit length and is defined by  $p = \sum_{n=1}^N (\frac{2n-1-N}{N-1}) (c_{n,A}^\dagger c_{n,A} + c_{n,B}^\dagger c_{n,B})$ . It, being proportional to the quantum mechanical position operator, is ill defined within periodic boundary conditions. Then, in the present section, we apply open boundary conditions and use a world-line QMC approach to compute equilibrium values of any quantum observable.

Consider the Hamiltonian without dissipation,

$$H_{\text{SSH}} = v \sum_{n=1}^N (c_{n,A}^\dagger c_{n,B} + c_{n,B}^\dagger c_{n,A}) + w \sum_{n=1}^{N-1} (c_{n+1,A}^\dagger c_{n,B} + c_{n,B}^\dagger c_{n+1,A}), \quad (3)$$

where  $n$  is the spatial coordinate of the cell and  $A, B$  denotes the site within cell. We make a Suzuki-Trotter decomposition, discretizing the imaginary time in  $2L$  steps of width  $\Delta\tau = \frac{\beta}{L}$  (the convergence with respect to  $\Delta\tau$  and  $N$  is discussed in detail in Appendix A). In Fig. 2 we show the case of  $N = 4$  cells (eight sites) and  $2L = 8$  time steps. The horizontal axis corresponds to the sites (spatial coordinate) while the vertical one corresponds to the imaginary time. The two terms of the Hamiltonian (intracell and intercell) act on alternating time

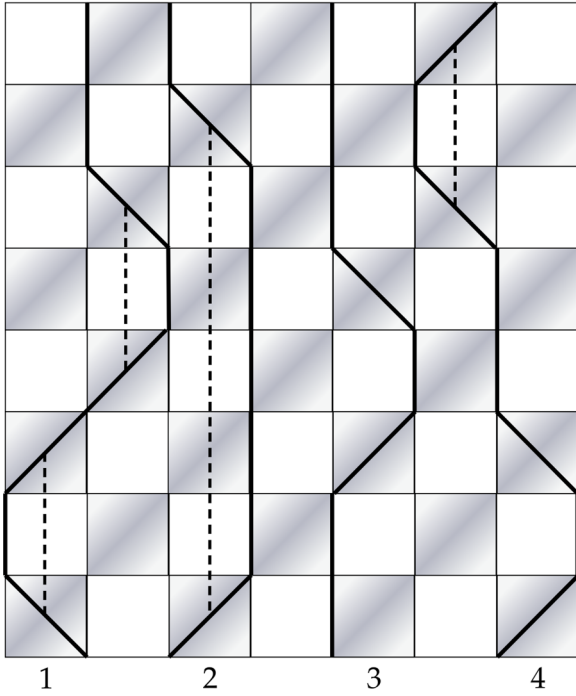


FIG. 2. Example of Suzuki-Trotter decomposition, for  $N = 4$  cells (eight sites) and  $2L = 8$  time steps. Bold-black lines represent the world-lines of four electrons, while dashed lines represent links between hoppings. The electrons hop only on the shaded plaquettes.

steps, corresponding to the shaded plaquettes of Fig. 2. So for example the term  $v(c_{1,A}^\dagger c_{1,B} + c_{1,B}^\dagger c_{1,A})$  acts only on the four shaded plaquettes in the leftmost column of Fig. 2, the term  $w(c_{1,B}^\dagger c_{2,A} + c_{2,A}^\dagger c_{1,B})$  on the four shaded plaquettes of the second leftmost column, and so on.

On each site of the square lattice obtained there is a variable  $n_{n,v,j} = 0, 1$ , where  $n = 1, \dots, N$  is the spatial coordinate of the cell,  $v = A, B$  denotes the site within cell, and  $j = 1, \dots, 2L$  the temporal coordinate, denoting the presence or absence of a particle. The occupied sites ( $n_{n,v,j} = 1$ ) form continuous lines (world-lines), shown as bold lines in Fig. 2, and particles can hop only where the corresponding term of the Hamiltonian acts, therefore only on the shaded plaquettes. Due to the cyclic property of the trace, periodic boundary conditions are applied on the temporal (vertical) coordinate, so that a particle must return at the final time at the initial position.

In the absence of dissipation, we use the normal loop algorithm to extract world-line configurations [48]. The mean values  $\langle H_v \rangle$  and  $\langle H_w \rangle$  turn out to be, respectively,  $-\beta^{-1} \langle n_{\text{hop}}^{(1)} \rangle$  and  $-\beta^{-1} \langle n_{\text{hop}}^{(2)} \rangle$ , where  $n_{\text{hop}}^{(1,2)}$  are the number of hoppings intracell (between  $n, A$  and  $n, B$ ) and intercell (between  $n, B$  and  $n+1, A$ ). At a given imaginary time  $j$ , the polarization is given by

$$p_j = \sum_{n=1}^N \left( \frac{2n-1-N}{N-1} \right) (n_{n,A,j} + n_{n,B,j}), \quad (4)$$

so that the polarization distribution  $P(p)$  can be computed from the values of  $p_j$  at each imaginary time and QMC step.

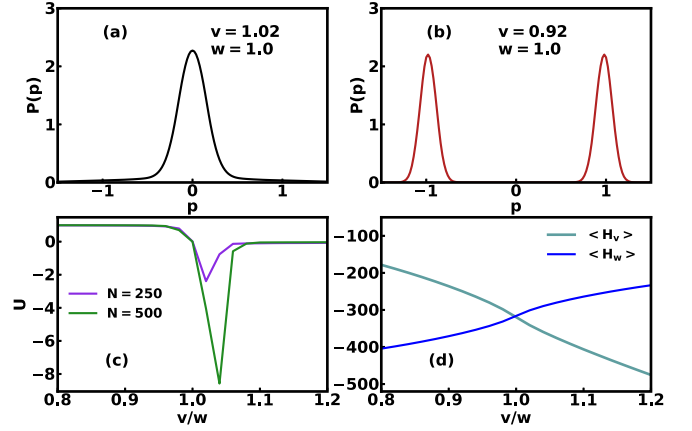


FIG. 3. [(a),(b)] Polarization probability distribution  $P(p)$  in the trivial and topological phases, respectively. (c) Binder parameter vs  $v/w$ ; (d) average values of  $H_v$  and  $H_w$  vs  $v/w$ . All plots refer to the noninteracting case with  $\beta = 100$  and  $\Delta\tau = 0.001$ .  $N = 500$  in (a), (b), and (d).

In the presence of the environment, we include a new set of variables, represented by links between two “hoppings”. A hopping corresponds to a shaded plaquette where an electron changes its position. The link between two hopping plaquette (shown as dashed bold lines in Fig. 2) represents the emission and absorption of a phonon, that changes the weight of the world-line by a factor  $\tilde{\omega}^{-2} K(\frac{\Delta\tau}{2} |j-j'|)$ , where  $1 \leq j, j' \leq 2L$  are the imaginary times of the plaquettes linked, and  $K(\tau) = \int d\omega J(\omega) \frac{\cosh[\omega(\frac{\beta}{2}-\tau)]}{\sinh(\beta\omega/2)}$  ( $K$  stems from the exact elimination of the bath degrees of freedom).

We alternate Metropolis-like moves on the links, and loop moves on the world-lines. When applying the loop algorithm, linked hopping plaquettes have to be “frozen”, because phonons cannot be emitted or absorbed on nonhopping plaquettes. This algorithm satisfies detailed balance and ergodicity, because the probability to remove all the links, make a “free” loop move (which is ergodic in the absence of the links), and then insert a different set of links, is larger than zero.

## B. QMC results: Polarization and Binder parameter as markers of topological phases

Now we prove that the polarization distribution  $P(p)$  can be used as marker of topological phase transition. To this aim, we analyze the behavior of  $P(p)$  in the bare SSH where it is well known that  $v = w$  represents the border between the trivial and topological insulating phases. In Fig. 3(a),  $v > w$ ,  $P(p)$  displays one peak centered at  $p = 0$ . In Fig. 3(b), i.e., within the topological phase ( $v < w$ ),  $P(p)$  acquires a bimodal character, with two peaks centered at  $p = \pm 1$ . The presence of two peaks, whose width becomes narrower and narrower by decreasing the temperature  $T$  and increasing  $N$ , signals the emergence of the edge states. In Fig. 3(c) we plot the Binder parameter  $U$  vs the ratio  $v/w$  for different lattice sizes.  $U = \frac{1}{2} (3 - \frac{\langle p^4 \rangle}{\langle p^2 \rangle^2})$  is the fourth-order cumulant of the distribution  $P(p)$  and, in statistical physics, is frequently used to determine accurately critical points. Similar to standard phase

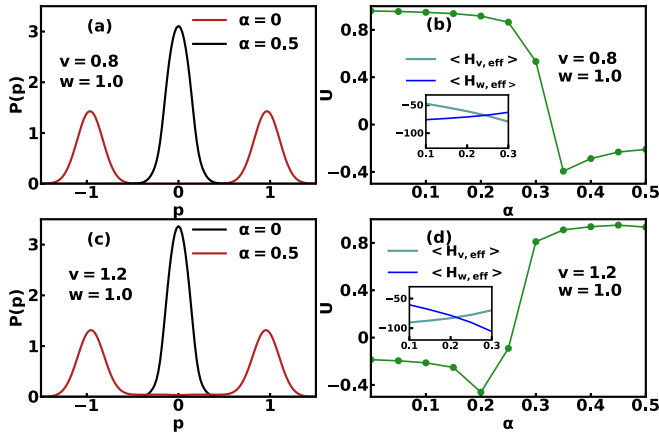


FIG. 4. Polarization probability distribution in (a) [(c)] and Binder parameter in (b) [(d)] vs  $\alpha$ , in the case of intracell [intercell] hopping coupled with local baths with  $N = 100$ ,  $\beta = 100$ , and  $\Delta\tau = 0.001$ . (Insets) Mean values of  $H_{v, \text{eff}}$  and  $H_{w, \text{eff}}$  vs  $\alpha$ .

transitions, the plots point out that the different curves cross at  $v = w$ , changing sign and exhibiting a minimum in the trivial phase, near the threshold, that is the typical behavior within first order discontinuous phase transitions. In Fig. 3(d) we plot the average values of the two terms of the Hamiltonian Eq. (1) vs  $v/w$ . As expected, in the thermodynamic limit, they cross at  $v = w$ , where the topological quantum phase transition sets in. These observations point out that, in order to identify the occurrence of the topological phase transition, it is possible to use the methods used in the statistical physics to characterize the phase transitions, although the key concepts of Landau classification, i.e., symmetry breaking and local order parameter, are missing in topological phase transitions, where gapless edge states appear and bulk properties show no changes.

Now the natural question is: What happens when the interaction with the environment is turned on? In Figs. 4(a) and 4(b) the plots of the probability distribution and the Binder parameter show that, if the coupling with local baths affects the intracell hopping, environment appears as detrimental for topological states of matter. Starting from a topological insulator,  $v < w$ , and increasing the strength of the coupling, a phase transition occurs towards a trivial insulator. On the other hand, if the interaction with the bosonic fields acts on the intercell transfer integrals, a topological phase transition is induced [see Figs. 4(c) and 4(d)]. Interestingly, the critical values of the fermion-boson coupling  $\alpha_c$  are in good agreement with the crossing points of the average values of the hopping terms, provided interaction contributions with the baths are included (see insets).

The explanatory phase diagrams, corresponding to intra- and intercell fermion-boson couplings, are reported in Figs. 5(a) and 5(b). They clearly show that in the former (latter) case the interactions with local baths is detrimental (favorable) for the emergence of the topology. In Fig. 5 we compare also the results obtained by considering classical and quantum oscillators in the local heat baths. Finally, one can show that also in the case of simultaneous coupling between intra- and intercell hopping and local baths (but with different

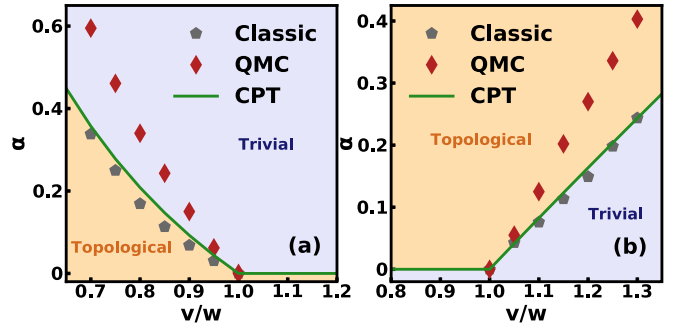


FIG. 5. Phase diagram, in the case of intra[inter]cell hopping coupled with local baths in (a) [(b)], for quantum [red diamonds] and classical bosons [grey points] through MC technique. Green line denotes the critical values of the couplings obtained through CPT for quantum baths.

coupling strength) it is possible to observe a topological phase transition. In the Appendix C we show the phase diagram referred to a particular choice of the hopping.

## IV. PERIODIC BOUNDARY CONDITIONS: TOPOLOGICAL INVARIANT AND NON-HERMITIAN PHYSICS

### A. Cluster perturbation theory (CPT)

In macroscopic systems, in general, one can assume also periodic boundary conditions. A system of this kind has no surface and all of its properties are by construction bulk ones. In this case the spontaneous polarization is related to the Berry phase and leads to the topological invariant  $\eta$ . Since the chiral symmetry is preserved,  $\eta$  can be evaluated by performing an integral over the Brillouin zone of the Green's function at zero frequency [49–53],

$$\eta = \frac{1}{4\pi i} \int_{-\pi}^{\pi} dk \text{Tr}\{\sigma_z G(k, 0) \partial_k G^{-1}(k, 0)\}, \quad (5)$$

where  $\sigma_z$  is the Pauli matrix. The CPT approach [44,45] represents a very straightforward approximation that generally applies to lattice models with local interactions. It is particularly precise in models where the local interaction is predominant. One starts by tiling the whole lattice into identical and finite-size clusters. Then one proceeds to solve these clusters exactly and connects them treating intercluster hopping amplitudes through perturbation theory. It represents a very smart tool to evaluate easily accurate Green's functions and, then, spectral functions. Naturally, the validity of the approach improves by increasing the size of the cluster. Here we consider a two site cluster: if the intra(inter)cell hoppings  $v$  ( $w$ ) are coupled with the local baths, the two cluster sites belong to the same (different) cell of the SSH chain. In this way, one obtains four mixed Green's functions,  $G_{i,j}(k, \omega)$  of the interacting system (indexes  $i$  and  $j$  can assume two values corresponding to the two cluster sites). These functions allow us to calculate the topological invariant via Eq. (5) disclosing the emergence of topological features. Usually the cluster Green's function is obtained through numerical approaches, such as the Lanczos method. Surprisingly we show that, by choosing as cluster two sites connected through an hopping coupled with a local environment, the cluster problem admits

an analytic solution (all calculations are presented in detail in Appendix E). The specific form of the cluster Green's function  $G_{CL}$  varies depending on the case under consideration. If the intracell hoppings  $v$  are coupled with the local baths (so  $\tilde{\omega} = v$ ), we have in general that  $c_1 = c_{n,A}$  and  $c_2 = c_{n,B}$ , i.e., the two sites of the cluster belong to the same cell of the SSH chain. As consequence in this case  $G_{CL}$  does not carry any dependence of the momentum  $k$ , but this dependence is entirely in the intercluster matrix  $t_{IC}$ , because different clusters are in different cells of the chain. On the contrary, if we refer to the case in which the intercell hoppings  $w$  are coupled with external baths, then the sites of the clusters belong to different cells of the SSH chain, i.e.,  $c_1 = c_{n,B}$ ,  $c_2 = c_{n+1,A}$ , meanwhile different clusters are connected through sites belonging to the same cells. In summary, the cluster Green's function and intercluster matrix ( $t_{IC}$ ) in the  $\omega$  and  $k$  space read as

$$G_{CL}^{(v)}(z) = \begin{bmatrix} G_{11}(z) & G_{12}(z) \\ G_{12}(z) & G_{11}(z) \end{bmatrix}, \quad t_{IC}^{(v)}(k) = \begin{bmatrix} 0 & we^{-ik} \\ we^{ik} & 0 \end{bmatrix} \quad (6)$$

and

$$G_{CL}^{(w)}(k, z) = \begin{bmatrix} G_{11}(z) & G_{12}(z)e^{-ik} \\ G_{12}(z)e^{ik} & G_{11}(z) \end{bmatrix}, \quad t_{IC}^{(w)} = \begin{bmatrix} 0 & v \\ v & 0 \end{bmatrix}, \quad (7)$$

where in the Appendix E we show that  $G_{11}(z) = G_{22}(z) = G^P(z) + G^B(z)$  and  $G_{12}(z) = G_{21}(z) = G^P(z) - G^B(z)$ ,

$$G^P(z) = -\frac{i}{2} e^{\frac{\tilde{\omega} + \alpha\tilde{\omega} - z}{\omega_D}} [i(\tilde{\omega} + \alpha\tilde{\omega} - z)]^{-1 + \frac{\alpha\tilde{\omega}}{\omega_D}} \times (i\omega_D)^{-\frac{\alpha\tilde{\omega}}{\omega_D}} \Gamma\left(1 - \frac{\alpha\tilde{\omega}}{\omega_D}, \frac{\tilde{\omega} + \alpha\tilde{\omega} - z}{\omega_D}\right) \quad (8)$$

and

$$G^B(z) = -\frac{i}{2} e^{\frac{\tilde{\omega} + \alpha\tilde{\omega} + z}{\omega_D}} [-i(\tilde{\omega} + \alpha\tilde{\omega} + z)]^{-1 + \frac{\alpha\tilde{\omega}}{\omega_D}} \times (-i\omega_D)^{-\frac{\alpha\tilde{\omega}}{\omega_D}} \Gamma\left(1 - \frac{\alpha\tilde{\omega}}{\omega_D}, \frac{\tilde{\omega} + \alpha\tilde{\omega} + z}{\omega_D}\right), \quad (9)$$

introducing the incomplete Gamma function  $\Gamma(a, x) = \int_x^\infty t^{a-1} e^{-t} dt$ .

Finally, the CPT Green's function is built in the following way:

$$[G_{CPT}^{(\tilde{\omega})}(k, z)]^{-1} = [G_{CL}^{(\tilde{\omega})}]^{-1} - t_{IC}^{(\tilde{\omega})}. \quad (10)$$

describing the full SSH chain interacting with local baths, under periodic boundary conditions. The Green's function  $G_{CPT}(k, z)$  represents the primary quantity of the CPT approach and allows us to obtain several observables. First of all, we emphasize that Green's functions obtained through CPT approach reduce naturally to that ones of the noninteracting limit for  $\alpha = 0$  (see Appendix D). In addition, this type of interacting SSH model preserves the chiral symmetry, established by the operator  $\sigma_z$  in the electronic space, so that we can evaluate the topological invariant  $\eta$  through Eq. (5) by means of zero-frequency component of Eq. (10).

It is straightforward to show that, independently of the kind of coupling considered, we have  $G_{11}(z = 0) = 0$  meanwhile

$G_{12}(z = 0)$  assumes a finite value depending only on  $\tilde{\omega}$  and the strength of the coupling  $\alpha$ .

If we focus on  $\tilde{\omega} = v$  and we define  $\tilde{v}(\alpha) = -1/G_{12}(z = 0)$ , by means of (5) and (10) we get

$$\eta^{(v)} = \frac{1}{2\pi} \int_{-\pi}^{\pi} dk \frac{we^{-ik}}{\tilde{v}(\alpha) + we^{-ik}}. \quad (11)$$

In the opposite case, when  $\tilde{\omega} = w$ , we find the following relation:

$$\eta^{(w)} = \frac{1}{2\pi} \int_{-\pi}^{\pi} dk \frac{\tilde{w}(\alpha)e^{-ik}}{v + \tilde{w}(\alpha)e^{-ik}}, \quad (12)$$

where, in an analogous way, we have defined  $\tilde{w}(\alpha) = -1/G_{12}(\omega = 0)$ .

The crucial points are: (i) at  $\alpha = 0$ ,  $-1/G_{12}(z = 0) = \tilde{\omega}$  and (ii)  $-1/G_{12}(z = 0)$  is an increasing monotonic function with  $\alpha$ . So, first of all, in the noninteracting case Eqs. (11) and (12) reduce to Eq. (D4). Furthermore, if we start from topological (trivial) state, characterized by  $v < w (v > w)$ , and consider the intra(inter)cell hopping coupled with the environment, by increasing the strength of the coupling with the bosonic fields  $\alpha$ , a topological phase transition from a topological (trivial) state to a trivial (topological) state sets in. In this way one obtains the phase diagram shown in Fig. 5.

### B. CPT results: Spectral functions and effective NHH

There are other Green's functions of physical interest,  $G_{+,+}(k, \omega)$ ,  $G_{-,-}(k, \omega)$ ,  $G_{-,+}(k, \omega)$ , and  $G_{+,-}(k, \omega)$  corresponding to the quasiparticle operators  $\gamma_{k,+}$ ,  $\gamma_{k,-}$  of the bare SSH model, in terms of which the Hamiltonian assumes the diagonal form  $H_{SSH} = \sum_k (E_{k,+} \gamma_{k,+}^\dagger \gamma_{k,+} + E_{k,-} \gamma_{k,-}^\dagger \gamma_{k,-})$  (see Appendix D). They provide detailed pieces of information on the renormalized band structure as well as spectral functions,  $A(k, \omega) = -\Im G(k, \omega)/\pi$ . Clearly, in the absence of fermion-boson coupling, the off diagonal Green's functions,  $G_{-,+}(k, \omega)$  and  $G_{+,-}(k, \omega)$ , vanish, whereas the spectral functions  $A_{-,-}(k, \omega)$  and  $A_{+,+}(k, \omega)$ , corresponding to the diagonal Green's function  $G_{-,-}(k, \omega)$  and  $G_{+,+}(k, \omega)$ , are delta functions centered at  $E_{k,-}$  and  $E_{k,+}$ , respectively. In Figs. 6(a) and 6(b) we plot the spectral weight functions  $A_{-,-}(k, \omega)$  and  $A_{+,+}(k, \omega)$  at  $k = \pi$  for the two considered models. In both cases, by increasing the coupling with local heat baths, the two main peaks become closer and closer and, at  $\alpha = \alpha_c$ , become coincident. For values  $\alpha > \alpha_c$ , the two peaks swap: a closure and reopening of the gap takes place. Note the presence of tails in the spectral functions due to the interactions that are associated with a corresponding reduction of the quasiparticle spectral weight. We highlight that the critical values of  $\alpha$ , determined through the observation of the discontinuous behavior of the topological invariant, align well with those obtained using the Monte Carlo technique when considering classical oscillators, i.e., employing mean-field theory for bosonic modes, in the local baths (see Appendix B). However, the CPT Green's function exhibits notable distinctions from those derived by considering classical bosons, especially by considering dynamical properties. Specifically, in the latter scenario, a mere trivial renormalization of the hopping associated with coupling occurs for every momentum value  $k$ . Consequently, the spectral functions manifest as trivial delta

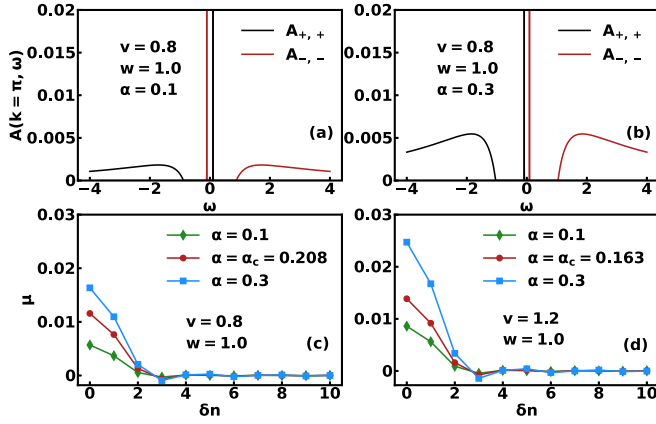


FIG. 6. [(a),(b)] Spectral functions  $A_{+,+}(k, \omega)$  and  $A_{-,-}(k, \omega)$  at  $k = \pi$  and couplings below (a) and above (b) the critical value  $\alpha_c$ , in the case of intracell hopping coupled with local baths. [(c),(d)] Effective sublattice hopping  $\mu$  vs cell distance  $\delta n$  for different interaction strengths (with  $0.1 < \alpha_c < 0.3$ ), for intra- and intercell fermion-boson couplings respectively.

peaks, lacking any indications of broadening or the presence of excitation tails at  $T = 0$ . This stands in contrast to the CPT Green's function that, as we will prove in the following, allows to introduce an effective NHH for the fermionic subsystem (see Appendix F for details). The first step is the determination of the poles of the  $2 \times 2$  matrix  $G_{\pm,\pm}(k, \omega)$  for any fixed value of  $k$ . They form two energy bands,  $-\tilde{E}_k - i\delta_k$  and  $\tilde{E}_k - i\delta_k$  with  $\delta_k \geq 0$ , i.e., the poles are located in the lower half plane. The effective Hamiltonian assumes diagonal form in the momentum space. Clearly, it is possible to express it in terms of creation and annihilation operators associated with Wannier function in the real space,  $H_{\text{eff}} = H_1 + H_2 + H_3$ , where

$$H_1 = -i \sum_{n,\delta n} \mu(|\delta n|) [c_{A,n+\delta n}^\dagger c_{A,n} + c_{B,n+\delta n}^\dagger c_{B,n} + \text{H.c.}], \quad (13)$$

$$H_2 = \sum_{n,\delta n} \tilde{v}(|\delta n|) [c_{A,n+\delta n}^\dagger c_{B,n} + c_{B,n}^\dagger c_{A,n+\delta n}], \quad (14)$$

and

$$H_3 = \sum_{n,\delta n} \tilde{w}(|\delta n| - 1) [c_{A,n+\delta n}^\dagger c_{B,n} + c_{B,n}^\dagger c_{A,n+\delta n}], \quad (15)$$

with  $\mu(\delta n) = \frac{1}{2\pi} \int_0^\pi dk \delta_k \cos[k\delta n]$ ,  $\tilde{v}(\delta n) = \frac{\tilde{v}}{\pi} \int_0^\pi dk \frac{\tilde{E}_k}{E_k} \cos[k\delta n]$ ,  $\tilde{w}(\delta n) = \frac{\tilde{w}}{\pi} \int_0^\pi dk \frac{\tilde{E}_k}{E_k} \cos[k\delta n]$ , where  $\tilde{v} = \tilde{v}(\alpha)$  ( $\tilde{v} = v$ ),  $\tilde{w} = w$  ( $\tilde{w} = \tilde{w}(\alpha)$ ) if the coupling with the bosonic field involves the intra- (inter)cell transfer integral. Finally  $E'_k = |\tilde{v} + \tilde{w}e^{-ik}|$  [the Appendix F contains the detailed derivation of the NHH, expressed as sum of Eqs. (13), (14), and (15)]. Here: (i)  $H_1$  (anti-Hermitian operator) describes an effective hopping of the fermions within the same sublattice (this contribution vanishes in the closed system) and (ii)  $H_2$  and  $H_3$  (Hermitian operators) represent the effective hopping between two sites, each of them being located in one of the two sublattices, whose distance is  $\delta n$ . Clearly in the absence of interaction,  $\tilde{E}_k = E_k$ ,  $\delta_k = 0$  and the only nonvanishing hoppings are  $\tilde{v}(0) = v$  and  $\tilde{w}(1) = w$ , i.e.,  $H_{\text{eff}}$  reduces itself to the bare SSH model. The plots in Figs. 6(c) and 6(d) show

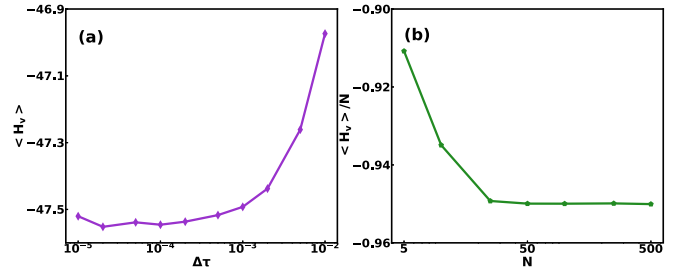


FIG. 7. Convergence tests of the QMC approach. (a) Mean value of  $H_v$  vs imaginary time step and (b) mean value of  $H_v/N$  vs number of cells  $N$ .

that, independently of the kind of coupling with local baths, by increasing the strength of the interaction, the absolute value of the magnitude of the quantity  $\mu(\delta n)$ , that is the main marker of the non-Hermiticity of the subsystem Hamiltonian, becomes larger and larger [54].

## V. CONCLUSIONS

We investigated, within the SSH model, the effects on the topological phase transitions induced by two different couplings with the environment. We proved that one of them can favor the emergence of topological features. Furthermore we demonstrated that (1) bimodality of the polarization distribution can be used as marker of the topological phase transition occurrence and (2) CPT provides an effective NHH for the subsystem: main source of the non-Hermiticity is given by a pure imaginary transfer integral within the same sublattice.

## ACKNOWLEDGMENTS

G.D.F. acknowledges financial support from PNRR MUR Project No. PE000023-NQSTI; N.N. is supported by JST CREST Grant No. JPMJCR1874, Japan. C.A.P. acknowledges funding from the IQARO (SpIn-orbitronic QuAntum bits in Reconfigurable 2D-Oxides) project of the European Union's Horizon Europe research and innovation programme under Grant Agreement No. 101115190. C.A.P. acknowledge funding from the PRIN 2022 PNRR project P2022SB73K - Superconductivity in KTaO3 Oxide-2DEG NANodevices for Topological quantum Applications (SONATA) financed by the European Union-Next Generation EU.

## APPENDIX A: QMC CONVERGENCE

We check the convergence of the observables with the step  $\Delta\tau$  of the Suzuki-Trotter approximation, computing the mean value of the energy for  $10^{-5} \leq \Delta\tau \leq 10^{-2}$ . For the value used in the paper,  $\Delta\tau = 10^{-3}$ , we get a result within the third decimal figure from the asymptotic value, as shown in Fig. 7(a). We also check the convergence with the number of cells  $N$ , as shown in Fig. 7(b). In this case, already for  $N = 50$  cells, the relative difference with the asymptotic value is less than  $10^{-3}$  (PBC were used).

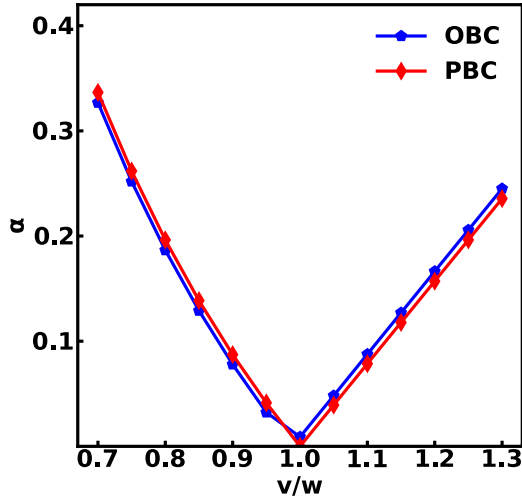


FIG. 8. Comparison between critical points obtained in the QMC approach with local baths of classical phonons under PBC and OBC.

### APPENDIX B: CLASSICAL OSCILLATORS

In the case of classical oscillators, the bath and interaction Hamiltonians can be written as

$$H_B + H_{SSH-B} = \sum_{\alpha,n} \frac{p_{\alpha,n}^2}{2m} + \sum_{\alpha,n} \frac{m\omega_\alpha^2}{2} x_{\alpha,n}^2 + \sum_{\alpha,n} g_{\alpha,n} \sqrt{\frac{2m\omega_\alpha}{\hbar}} x_{\alpha,n} H_{hop,n}, \quad (B1)$$

where  $m$  is the mass of the oscillators,  $p_{\alpha,n}$  the momentum, and  $x_{\alpha,n}$  the position. As  $p_{\alpha,n}$  and  $x_{\alpha,n}$  commute, in the partition function the integral over momentum variables can be factorized and is irrelevant for the computation of other observables. The trace over electronic degrees of freedom can be computed for fixed values of the positions  $x_{\alpha,n}$ , and the ground-state energy

$$E(\{x_{\alpha,n}\}) = \sum_{\alpha,n} \frac{m\omega_\alpha^2}{2} x_{\alpha,n}^2 - \lim_{T \rightarrow 0} k_B T \ln \text{Tr}(e^{-\beta H_{SSH-B}}) \quad (B2)$$

can be computed. Then,  $E(\{x_{\alpha,n}\})$  can be minimized with respect to the positions  $x_{\alpha,n}$ , obtaining

$$m\omega_\alpha^2 x_{\alpha,n} = g_{\alpha,n} \sqrt{\frac{2m\omega_\alpha}{\hbar}} X_n, \quad (B3)$$

where  $X_n$  depends only on the cell. Substituting back in the Hamiltonian, we obtain that

$$H_B + H_{SSH-B} = \sum_n \frac{\mu_n}{2} X_n^2 + \sum_n \mu_n X_n H_{hop,n}, \quad (B4)$$

where  $X_n$  are the values that minimize the ground-state energy, and  $\mu_n = 2 \sum_\alpha \frac{g_{\alpha,n}^2}{\hbar\omega_\alpha} = 2 \int d\omega \frac{J(\omega)}{\omega}$ . All the observables can then be computed using the effective Hamiltonian (B4). By considering the local baths as set of classical oscillators (or in an equivalently way by considering mean-field theory for bosons), one is able to compare the critical points obtained under OBC and PBC. The results are shown in Fig. 8, pointing

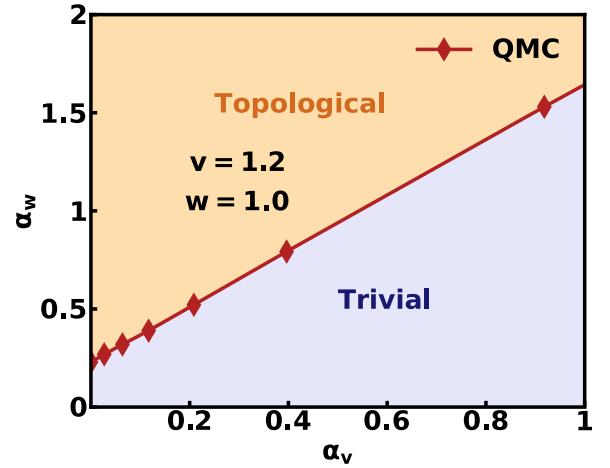


FIG. 9. Phase diagram resulting by QMC simulation in the case of intra- and intercell hopping simultaneously coupled with local baths with different strengths, in the case  $w < v$ .

out how the topological phase transition is almost unaffected by the choice of boundary conditions made.

### APPENDIX C: SIMULTANEOUS COUPLING OF INTRA- AND INTER CELL HOPPING WITH THE ENVIRONMENT

In order to show the robustness of the physics stressed in the Sec. III, we perform further QMC simulations considering the intracell hopping  $v$  and intercell hopping  $w$  simultaneously coupled with the environment, with in general different coupling strength  $\alpha_v$  and  $\alpha_w$ , respectively. In Fig. 9 we analyze the case with  $v = 1.2$  and  $w = 1.0$ . The fundamental point is the following: by starting from the condition  $v > w$  ( $w > v$ ) and fixed the value of the coupling  $\alpha_v$  ( $\alpha_w$ ), there exists a greater value of  $\alpha_w > \alpha_v$  ( $\alpha_v > \alpha_w$ ) such that the system runs into a topological phase transition. It is important to stress that in general to obtain a topological phase transition the intra- and intercell hoppings have to interact with the environment with different strengths.

### APPENDIX D: THE BARE SSH CHAIN

We start by recalling the main physical quantities for a noninteracting SSH chain, in order to further stress how the phononic interaction affects them.

The Hamiltonian of the bare SSH model is well known in the literature of topological insulators,

$$H_{SSH} = v \sum_{n=1}^N c_{n,A}^\dagger c_{n,B} + w \sum_{n=1}^{N-1} c_{n+1,A}^\dagger c_{n,B} + \text{H.c.} \quad (D1)$$

Here  $c_{n,v}$  ( $c_{n,v}^\dagger$ ) destroys (creates) an electron in the site  $v = A, B$  of the  $n$ th cell, and  $v$  ( $w$ ) denotes the intra(inter)cell hopping. In the following, we will adopt periodic boundary conditions and use units such that  $\hbar = a = e = k_B = 1$ ;  $a$ ,  $e$ , and  $k_B$  being the lattice parameter, the electronic charge, and Boltzmann constant, respectively.

In terms of the Fourier transform of fermionic operators in the  $k$  space,

$$\begin{aligned} a_k &= \frac{1}{\sqrt{N}} \sum_n e^{-ikn} c_{A,n} \\ b_k &= \frac{1}{\sqrt{N}} \sum_n e^{-ikn} c_{B,n}, \end{aligned} \quad (\text{D2})$$

where  $k$  belongs to the first Brillouin zone (BZ), the Hamiltonian reads as

$$H(k) = v \sum_{k \in \text{BZ}} (a_k^\dagger b_k + \text{H.c.}) + w \sum_{k \in \text{BZ}} (e^{ik} a_k^\dagger b_k + \text{H.c.}) \quad (\text{D3})$$

Then, we can define four retarded Green's functions,  $G_{A,A}^{\text{SSH}}(k, t) = -i\theta(t) \langle \{a_k(t), a_k^\dagger(0)\} \rangle$ ,  $G_{B,B}^{\text{SSH}}(k, t) = -i\theta(t) \langle \{b_k(t), b_k^\dagger(0)\} \rangle$ ,  $G_{A,B}^{\text{SSH}}(k, t) = -i\theta(t) \langle \{a_k(t), b_k^\dagger(0)\} \rangle$ , and  $G_{B,A}^{\text{SSH}}(k, t) = -i\theta(t) \langle \{b_k(t), a_k^\dagger(0)\} \rangle$ . Here the symbol  $\{c, d\}$  indicates the anticommutator between the operators  $c$  and  $d$ .

This simple toy model underlines the main physical features of topological insulators at half filling. When open boundary conditions are adopted, the trivial insulating phase is obtained for  $v > w$ , whereas the topological phase, characterized by the appearance of gap-less edge states, sets in at  $v < w$ . On the other hand, in the thermodynamic limit and assuming periodic boundary conditions, the topological transition is marked by a topological invariant  $\eta$  that assumes a nonvanishing value in a discontinuous way. In the case of a bare SSH chain it reads as

$$\eta = \frac{1}{2\pi} \int_{-\pi}^{\pi} dk \frac{w e^{-ik}}{v + w e^{-ik}}. \quad (\text{D4})$$

The quantity  $\eta$  is zero for  $v > w$  indicating a trivial phase, while assumes a value equal to 1 in the topological phase for  $v < w$ . The topological transition from a trivial state to a topological state is signalled not only by the appearance of the edge states, but it is also accompanied by the closure of the energy gap, that happens precisely at  $k = \pm\pi$ .

The Hamiltonian in Eq. (D3) can be easily diagonalized by means of the quasiparticle basis  $\{\gamma_{k,+}, \gamma_{k,-}\}$ , defined as

$$\begin{aligned} \gamma_{k,+} &= \frac{1}{\sqrt{2}} [a_k + (n_x(k) - i n_y(k)) b_k] \\ \gamma_{k,-} &= \frac{1}{\sqrt{2}} [(n_x(k) + i n_y(k)) a_k - b_k], \end{aligned} \quad (\text{D5})$$

where  $n_x(k) = (v + w \cos k)/E_k$  and  $n_y(k) = w \sin k/E_k$ .

After this unitary transformation, the Hamiltonian assumes the diagonal form

$$H(k) = \sum_k (E_k \gamma_{k,+}^\dagger \gamma_{k,+} - E_k \gamma_{k,-}^\dagger \gamma_{k,-}), \quad (\text{D6})$$

where  $E_k = \sqrt{v^2 + w^2 + 2vw \cos k}$ . In particular  $-E_k$  and  $E_k$  are the eigenvalues of (D3), which describe the two bands of the topological insulator.

Analogously we can define the retarded Green's function associated with the quasiparticles  $G_{\mu\nu}(k, t) = -i\theta(t) \langle \{\gamma_{k,\mu}(t), \gamma_{k,\nu}^\dagger\} \rangle$ , with  $\mu, \nu = \pm$ . It is trivial to obtain the following relations in the frequency space:

$$\begin{aligned} G_{+,+}(k, z) &= \frac{1}{2} [(n_x(k) + i n_y(k)) G_{A,B}^{\text{SSH}}(k, z) \\ &\quad + (n_x(k) - i n_y(k)) G_{B,A}^{\text{SSH}}(k, z) + 2G_{A,A}^{\text{SSH}}(k, z)] \end{aligned} \quad (\text{D7})$$

and

$$\begin{aligned} G_{-,-}(k, z) &= \frac{1}{2} [-(n_x(k) + i n_y(k)) G_{A,B}^{\text{SSH}}(k, z) \\ &\quad - (n_x(k) - i n_y(k)) G_{B,A}^{\text{SSH}}(k, z) + 2G_{A,A}^{\text{SSH}}(k, z)]. \end{aligned} \quad (\text{D8})$$

In particular,  $G_{+,+}(k, z) = \frac{1}{z - E_k}$ ,  $G_{-,-}(k, z) = \frac{1}{z + E_k}$ , and  $G_{+,-}(k, z) = G_{-,+}(k, z) = 0$ . Here  $z = \omega + i\delta$ , with  $\delta > 0$  ( $z$  lies in the upper half plane).

Finally, by performing the limit  $\delta \rightarrow 0$ , we can build up the spectral functions, that describe two delta functions peaked at  $\omega = \pm E_k$ ,

$$A_{\pm,\pm}(k, \omega) = -\frac{1}{\pi} \Im G_{\pm,\pm}(k, \omega) = \delta(\omega \mp E_k). \quad (\text{D9})$$

We naturally expect that interactions with local baths not only generate the broadening of these peaks, but also tails due to the phononic excitations.

Finally, one can define the DOS related to the two energy-bands  $\pm E_k$  of the insulators,

$$\text{DOS}(\omega)_+ = \int_{-\pi}^{\pi} dk \frac{1}{2\pi} A_{+,+}(k, \omega) \quad (\text{D10})$$

and

$$\text{DOS}(\omega)_- = \int_{-\pi}^{\pi} dk \frac{1}{2\pi} A_{-,-}(k, \omega). \quad (\text{D11})$$

## APPENDIX E: THE CLUSTER PROBLEM

In this Appendix we will prove that the Green's function of the cluster problem admits an analytic solution.

Our starting point is the following cluster Hamiltonian, describing two sites (labelled by  $i = 1, 2$ ) connected through an hopping interacting with a local environment,

$$H = \tilde{\omega} C + C \sum_{\alpha} g_{\alpha} (b_{\alpha} + b_{\alpha}^{\dagger}) + \sum_{\alpha} \omega_{\alpha} b_{\alpha}^{\dagger} b_{\alpha}, \quad (\text{E1})$$

where  $C = c_1^{\dagger} c_2 + c_2^{\dagger} c_1$  and  $\tilde{\omega}$  denotes the hopping within the cluster. In particular,  $\tilde{\omega} = v$  ( $\tilde{\omega} = w$ ) if the coupling with the bosonic field regards the intra(inter)cell transfer integral.

The problem associated to this type of Hamiltonian can be solved analytically, in similar way to the independent boson model. Indeed, we have that  $[C, H] = 0$ . Then, we can consider the following unitary operator  $U = \exp(C\Omega)$ , where  $\Omega = \sum_{\alpha} \frac{g_{\alpha}}{\omega_{\alpha}} (b_{\alpha} - b_{\alpha}^{\dagger})$ .

A generic operator transforms under  $U$  with the Baker-Campbell-Hausdorff formula  $\tilde{A} = \exp(S)A \exp(-S) = A + [S, A] + [S, [S, A]]/2! + \dots$ . As a consequence we have that  $\tilde{C} = C$ ,  $\tilde{b}_{\alpha} = b_{\alpha} - (g_{\alpha}/\omega_{\alpha})C$  and  $\tilde{b}_{\alpha}^{\dagger} = b_{\alpha}^{\dagger} - (g_{\alpha}/\omega_{\alpha})C$ . Finally, the transformed Hamiltonian  $\tilde{H} = U^{\dagger} H U$  reads as

$$\tilde{H} = \tilde{\omega}C - E_R C^2 + \sum_{\alpha} \omega_{\alpha} b_{\alpha}^{\dagger} b_{\alpha}, \quad (\text{E2})$$

where we have defined  $E_R = \sum_{\alpha} (g_{\alpha}^2/\omega_{\alpha})$ .

Now, we only need the eigenvalues and eigenstates of  $\tilde{H}$ , by considering the subsectors of 0, 1, and 2 particles. In particular for 0 and 2 particles we have that  $C|0_A, 0_B\rangle = 0$  and  $C|1_A, 1_B\rangle = 0$ , then in these subsectors we have  $\tilde{H} = \sum_{\alpha} \omega_{\alpha} b_{\alpha}^{\dagger} b_{\alpha}$ , i.e., the spectrum of free phonons. By considering the sector of 1 particle, we have that the electronic eigenvectors are  $|\psi_{\pm}\rangle_{el} = (c_1^{\dagger} \pm c_2^{\dagger})|0_1, 0_2\rangle/\sqrt{2}$ .

We consider the half-filling case, so the ground state of the original Hamiltonian, Eq. (E1), reads as  $|\psi_0\rangle = U|\psi_{-}\rangle_{el}|0_1, \dots, 0_M\rangle_{ph}$ , where  $M$  indicates the number of harmonic oscillators describing the bath.

Our purpose is to evaluate the retarded Green's functions  $G_{ij}^R(t) = -i\theta(t)\langle\psi_0|c_i(t), c_j^{\dagger}(0)|\psi_0\rangle$ , with  $i, j = 1, 2$ . In particular, it is convenient to consider the Lehmann

representation in the space of frequencies,

$$\begin{aligned} G_{ij}^R(\omega + i\delta) &= \sum_m \frac{\langle\psi_0^{(N)}|c_i|\psi_m^{(N+1)}\rangle\langle\psi_m^{(N+1)}|c_j^{\dagger}|\psi_0^{(N)}\rangle}{\omega + (E_0^{(N)} - E_m^{(N+1)}) + i\delta} \\ &+ \sum_n \frac{\langle\psi_0^{(N)}|c_j^{\dagger}|\psi_n^{(N-1)}\rangle\langle\psi_n^{(N-1)}|c_i|\psi_0^{(N)}\rangle}{\omega - (E_0^{(N)} - E_n^{(N-1)}) + i\delta} \\ &= G_{ij}^{(N)-(N+1)}(\omega + i\delta) + G_{ij}^{(N)-(N-1)}(\omega + i\delta), \end{aligned} \quad (\text{E3})$$

where, in our case,  $G_{ij}^R(\omega + i\delta) = G_{ij}^{1-2}(\omega + i\delta) + G_{ij}^{1-0}(\omega + i\delta)$  (particle and hole contributions), given by the following relations:

$$G_{ij}^{1-2}(\omega + i\delta) = \sum_m \frac{\langle\psi_0|c_i|\psi_m^{(2)}\rangle\langle\psi_m^{(2)}|c_j^{\dagger}|\psi_0\rangle}{\omega + (E_0 - E_m^{(2)}) + i\delta} \quad (\text{E4})$$

and

$$G_{ij}^{1-0}(\omega + i\delta) = \sum_n \frac{\langle\psi_0|c_j^{\dagger}|\psi_m^{(0)}\rangle\langle\psi_m^{(0)}|c_i|\psi_0\rangle}{\omega - (E_0 - E_m^{(0)}) + i\delta}. \quad (\text{E5})$$

Here  $|\psi_m^{(0)}\rangle = U|0_1, 0_2\rangle_{el}|u_1, \dots, u_M\rangle_{ph}$ ,  $|\psi_m^{(2)}\rangle = U|1_1, 1_2\rangle_{el}|u_1, \dots, u_M\rangle_{ph}$ ,  $E_m^{(0)} = E_m^{(2)} = \sum_l \omega_l u_l$ ,  $u_{\alpha}$  being the number of phonons with energy  $\omega_{\alpha}$  and  $E_0 = -\tilde{\omega} - E_R$  is the energy of the ground state at half filling.

By evaluating all the bra-ket products, it is straightforward to show that  $G_{ij}^{1-2}(\omega + i\delta) = G^P(\omega + i\delta)$  and  $G_{ij}^{1-0}(\omega + i\delta) = (2\delta_{ij} - 1)G^B(\omega + i\delta)$ , where we have defined

$$\begin{aligned} G^P(\omega + i\delta) &= \frac{1}{2} \sum_{\mu_1 \dots \mu_M} \left( e^{-S_1} \frac{S_1^{\mu_1}}{\mu_1!} \right) \dots \left( e^{-S_M} \frac{S_M^{\mu_M}}{\mu_M!} \right) \frac{1}{\omega + [-\tilde{\omega} - E_R - (\omega_1 \mu_1 + \dots + \omega_M \mu_M)] + i\delta}, \\ G^B(\omega + i\delta) &= \frac{1}{2} \sum_{\mu_1 \dots \mu_M} \left( e^{-S_1} \frac{S_1^{\mu_1}}{\mu_1!} \right) \dots \left( e^{-S_M} \frac{S_M^{\mu_M}}{\mu_M!} \right) \frac{1}{\omega - [-\tilde{\omega} - E_R - (\omega_1 \mu_1 + \dots + \omega_M \mu_M)] + i\delta}, \end{aligned}$$

with  $S_{\alpha} = g_{\alpha}^2/\omega_{\alpha}^2$ .

As a consequence we have that  $G_{11}(\omega + i\delta) = G_{22}(\omega + i\delta) = G^P(\omega + i\delta) + G^B(\omega + i\delta)$  and  $G_{12}(\omega + i\delta) = G_{21}(\omega + i\delta) = G^P(\omega + i\delta) - G^B(\omega + i\delta)$ .

The next step is looking for analytic expressions for  $G^P(\omega + i\delta)$  and  $G^B(\omega + i\delta)$ . By considering that  $(\omega + i\delta)^{-1} = -i \int_0^{\infty} e^{i(\omega+i\delta)t} dt$ , we can rewrite  $G^P(\omega + i\delta)$  and  $G^B(\omega + i\delta)$  in the following integral forms:

$$G^P(\omega + i\delta) = -\frac{i}{2} \int_0^{\infty} dt e^{-f(\omega, t)}$$

and

$$G^B(\omega + i\delta) = -\frac{i}{2} \int_0^{\infty} dt e^{-g(\omega, t)},$$

where

$$f(\omega, t) = \sum_{\alpha} S_{\alpha} (1 - e^{-i\omega_{\alpha} t}) e^{-\delta t} e^{i(\omega - \tilde{\omega} - E_R)t}$$

and

$$g(\omega, t) = \sum_{\alpha} S_{\alpha} (1 - e^{i\omega_{\alpha} t}) e^{-\delta t} e^{i(\omega + \tilde{\omega} + E_R)t}.$$

Now, it is convenient to perform the limit from a discrete set of frequencies  $\{\omega_{\alpha}\}$  to a continuum  $\sum_{\alpha} g_{\alpha}^2 f[\{\omega_{\alpha}\}] \rightarrow \int_0^{\infty} d\omega J(\omega) f(\omega)$ , where we define the bath spectral function  $J(\omega)$  as

$$J(\omega) = \alpha \tilde{\omega} \frac{\omega}{\omega_D} e^{-\omega/\omega_D} \quad (\text{E6})$$

that corresponds to the Ohmic case, and  $\omega_D$  is a cutoff frequency (it represents the largest energy scale). Then by passing to the continuum  $E_R = \sum_{\alpha} (g_{\alpha}^2/\omega_{\alpha}) \rightarrow \alpha \tilde{\omega}$  and by solving the integrals in the frequency, we get the following expressions:

$$\begin{aligned} G^P(\omega + i\delta) &= -\frac{i}{2} \int_0^{\infty} e^{-\frac{\alpha \tilde{\omega}}{\omega_D} \log(i\omega_D t + 1)} e^{-\delta t} e^{i(\omega - (\alpha + 1)\tilde{\omega})t} dt, \\ G^B(\omega + i\delta) &= -\frac{i}{2} \int_0^{\infty} e^{-\frac{\alpha \tilde{\omega}}{\omega_D} \log(-i\omega_D t + 1)} e^{-\delta t} e^{i(\omega + (\alpha + 1)\tilde{\omega})t} dt. \end{aligned}$$

Finally, after performing integrals with respect to the time, we obtain

$$G^P(\omega + i\delta) = -\frac{i}{2} e^{\frac{\tilde{\omega} + \alpha\tilde{\omega} - i\delta - \omega}{\omega_D}} [i(\tilde{\omega} + \alpha\tilde{\omega} - i\delta - \omega)]^{-1 + \frac{\alpha\tilde{\omega}}{\omega_D}} \\ \times (i\omega_D)^{-\frac{\alpha\tilde{\omega}}{\omega_D}} \Gamma\left(1 - \frac{\alpha\tilde{\omega}}{\omega_D}, \frac{\tilde{\omega} + \alpha\tilde{\omega} - i\delta - \omega}{\omega_D}\right)$$

and

$$G^B(\omega + i\delta) = -\frac{i}{2} e^{\frac{\tilde{\omega} + \alpha\tilde{\omega} + i\delta + \omega}{\omega_D}} [-i(\tilde{\omega} + \alpha\tilde{\omega} + i\delta + \omega)]^{-1 + \frac{\alpha\tilde{\omega}}{\omega_D}} \\ \times (-i\omega_D)^{-\frac{\alpha\tilde{\omega}}{\omega_D}} \Gamma\left(1 - \frac{\alpha\tilde{\omega}}{\omega_D}, \frac{\tilde{\omega} + \alpha\tilde{\omega} + i\delta + \omega}{\omega_D}\right),$$

where we have introduced the incomplete Gamma function  $\Gamma(a, x) = \int_x^\infty t^{a-1} e^{-t} dt$ .

#### APPENDIX F: EFFECTIVE NON-HERMITIAN SSH HAMILTONIAN

Beyond the Hermitian topological Hamiltonian, stemming from Green's function evaluated at zero frequency and useful to calculate the topological invariant, it is possible to introduce a non-Hermitian Hamiltonian by using the poles of the Green's function, i.e., by calculating the Green's function at no vanishing frequency in the half lower complex plane. This NHH captures the quasiparticle physics. To this aim, first of all we consider the Green's functions in the quasiparticle basis of operators (D5),

$$G_{+,+}(k, z) = \frac{1}{2} [(n_x(k) + in_y(k))G_{AB}^{CPT}(k, z) \\ + (n_x(k) - in_y(k))G_{BA}^{CPT}(k, z) + 2G_{AA}^{CPT}(k, z)], \quad (F1)$$

$$G_{-,-}(k, z) = \frac{1}{2} [-(n_x(k) + in_y(k))G_{AB}^{CPT}(k, z) \\ - (n_x(k) - in_y(k))G_{BA}^{CPT}(k, z) + 2G_{AA}^{CPT}(k, z)], \quad (F2)$$

$$G_{-,+}(k, z) = \frac{(n_x(k) + in_y(k))^2 G_{AB}^{CPT}(k, z) - G_{BA}^{CPT}(k, z)}{2}, \quad (F3)$$

and

$$G_{+,-}(k, z) = \frac{(n_x(k) - in_y(k))^2 G_{BA}^{CPT}(k, z) - G_{AB}^{CPT}(k, z)}{2}. \quad (F4)$$

In particular, we emphasize that, in general, in the presence of fermion-boson interaction, the Green's functions  $G_{+,+}(k, z)$  and  $G_{-,-}(k, z)$  are different from zero.

Next step is to look for the poles of the quasiparticles Green's functions. In general, with no zero interaction, the poles form two energy bands  $-\tilde{E}_k - i\delta_k$  and  $\tilde{E}_k - i\delta_k$ , with  $\delta_k > 0$ . Here  $\tilde{E}_k$  represents a renormalization of the bare spectrum and  $\delta_k$  is associated to a finite lifetime of quasiparticle. The typical behavior of  $-\delta_k$  vs  $\tilde{E}_k$  is shown in Fig. 10.

The eigenvectors corresponding to the eigenvalues  $\pm\tilde{E}_k - i\delta_k$  are  $|\pm\rangle = (\pm \exp(-i\phi(k)), 1)/\sqrt{2}$ . with

$$\tilde{\phi}(k) = \arctan\left(\frac{\tilde{w} \sin k}{\tilde{v} + \tilde{w} \cos k}\right), \quad (F5)$$

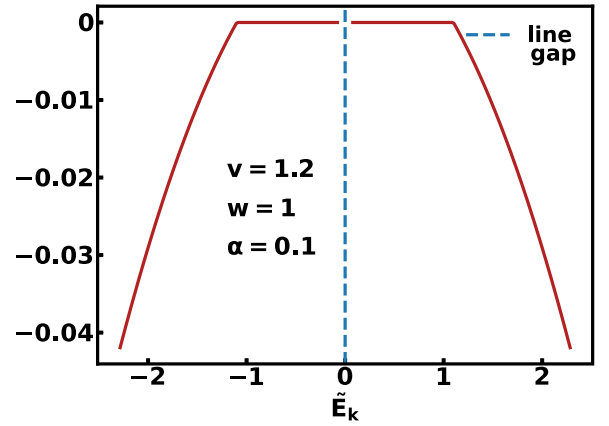


FIG. 10. Complex line-gapped energy spectrum obtained for  $\alpha = 0.1$ , in the case of intercell coupling with local baths.

where  $\tilde{v} = -1/G_{12}(z=0)$  ( $\tilde{v} = v$ ) and  $\tilde{w} = w$  ( $\tilde{w} = -1/G_{12}(z=0)$ ) if the coupling with the bosonic field involves the intra(inter)cell transfer integral.

In order to obtain the Hamiltonian in the  $k$ -space we perform the matrix product  $H(k) = P_k D_k P_k^{-1}$ , where  $P_k$  is the matrix that has as columns the two eigenvectors, i.e.,  $P_k = (|-\rangle, |+\rangle)$ , and  $D_k$  is the diagonal matrix with elements  $\pm\tilde{E}_k - i\delta_k$ . The result is

$$H_{\text{eff}}(k) = \begin{bmatrix} -i\delta_k & \tilde{E}_k e^{-i\phi(k)} \\ \tilde{E}_k e^{i\phi(k)} & -i\delta_k \end{bmatrix}, \quad (F6)$$

$$H_{\text{eff}} = \sum_k [a_k^\dagger \quad b_k^\dagger] H(k) \begin{bmatrix} a_k \\ b_k \end{bmatrix}. \quad (F7)$$

One can show that the quasiparticle Hamiltonian (F6) is able to reproduce the CPT Green's function of Eq. (10) thanks to the relation  $G_{CPT}(k, z) = [z - H(k)]^{-1}$ . Moreover, Eq. (F6) reduces to Eq. (D3) in the noninteracting limit ( $\delta_k \rightarrow 0$ ,  $\tilde{E}_k \rightarrow E_k$ ,  $\tilde{E}_k \exp\{-i\tilde{\phi}(k)\} \rightarrow v + w \exp\{-ik\}$ ). Then, one can write Eq. (F7) in the following explicit form:

$$H = -i \sum_k \delta_k [a_k^\dagger a_k + b_k^\dagger b_k] + \sum_k (e^{-i\tilde{\phi}(k)} \tilde{E}_k a_k^\dagger b_k + \text{H.c.}). \quad (F8)$$

The factor  $e^{-i\tilde{\phi}(k)}$  can be rewritten as

$$e^{-i\tilde{\phi}(k)} = \frac{\tilde{v} + \tilde{w} e^{-ik}}{|\tilde{v} + \tilde{w} e^{-ik}|} = \frac{\tilde{v} + \tilde{w} e^{-ik}}{E'_k}, \quad (F9)$$

and, consequently, the total effective Hamiltonian turns out to be the sum of three contributions,

$$H = -i \sum_k \delta_k [a_k^\dagger a_k + b_k^\dagger b_k] + v \sum_k \frac{\tilde{E}_k}{E'_k} (a_k^\dagger b_k + \text{H.c.}) \\ + w \sum_k \frac{\tilde{E}_k}{E'_k} (e^{-ik} a_k^\dagger b_k + \text{H.c.}). \quad (F10)$$

Now we apply the inverse transformation of the quasiparticle relation in order to write this effective Hamiltonian in the real space, i.e., in terms of the cell operators  $c_{A,n}, c_{B,n}$ . Let us focus for the moment on the first term of the Hamiltonian (F10),

i.e.,  $H_1 = -i \sum_k \delta_k [a_k^\dagger a_k + b_k^\dagger b_k]$ . We can perform the reverse transformation of (D2), obtaining

$$H_1 = -\frac{i}{N} \sum_k \delta_k \sum_{n,m} e^{ik(m-n)} (c_{A,m}^\dagger c_{A,n} + c_{B,m}^\dagger c_{B,n}). \quad (\text{F11})$$

Then, in the thermodynamic limit, i.e.,  $N \rightarrow \infty$ , it is convenient to pass from discrete sums in the wavevector  $k$  to integrals, i.e.,  $\sum_k(\dots) \rightarrow N/2\pi \int_{-\pi}^{\pi} dk(\dots)$ ,

$$H_1 = -i \sum_{n,m} (c_{A,m}^\dagger c_{A,n} + c_{B,m}^\dagger c_{B,n}) \left( \frac{1}{2\pi} \int_{-\pi}^{\pi} dk \delta_k e^{ik(m-n)} \right). \quad (\text{F12})$$

Finally, since  $\delta_k = \delta_{-k}$ ,  $H_1$  assumes the final form

$$H_1 = -i \sum_{n,\delta n} \mu(|\delta n|) [c_{A,n+\delta n}^\dagger c_{A,n} + c_{B,n+\delta n}^\dagger c_{B,n} + \text{H.c.}], \quad (\text{F13})$$

with

$$\mu(|\delta n|) = \frac{1}{2\pi} \int_0^\pi dk \delta_k \cos[\delta n k]. \quad (\text{F14})$$

Then, we can consider the last two terms of Eq. (F10),

$$H_2 = \tilde{v} \sum_k \frac{\tilde{E}_k}{E'_k} (a_k^\dagger b_k + \text{H.c.}) \quad (\text{F15})$$

and

$$H_3 = \tilde{w} \sum_k \frac{\tilde{E}_k}{E'_k} (e^{-ik} a_k^\dagger b_k + \text{H.c.}). \quad (\text{F16})$$

By repeating the same mathematical steps performed for  $H_1$ , we obtain

$$H_2 = \sum_{n,m} \tilde{v}(|m-n|) [c_{A,m}^\dagger c_{B,n} + c_{B,n}^\dagger c_{A,m}], \quad (\text{F17})$$

$$H_3 = \sum_{n,m} \tilde{w}(|m-n|-1) [c_{A,m}^\dagger c_{B,n} + c_{B,n}^\dagger c_{A,m}], \quad (\text{F18})$$

with

$$\tilde{v}(\delta n) = \frac{\tilde{v}}{\pi} \int_0^\pi dk \frac{\tilde{E}_k}{E'_k} \cos[\delta n k] \quad (\text{F19})$$

and

$$\tilde{w}(\delta n) = \frac{\tilde{w}}{\pi} \int_0^\pi dk \frac{\tilde{E}_k}{E'_k} \cos[\delta n k]. \quad (\text{F20})$$

Thanks to the CPT technique, we are able to discern the main effects manifested in the effective non-Hermitian Hamiltonian. In particular, the fermion-boson interaction generates a manifestly non-Hermitian sublattice hopping  $\mu(m-n)$  that gives rise also to an on-site potential when  $n=m$ . We emphasize that the sublattice potential  $\mu(m-n)$  and the generalized intra- and intercell hopping  $\tilde{v}(m-n)$ ,  $\tilde{w}(m-n)$  go to zero naturally when the cells considered are very far from each other, i.e.,  $|(n-m)| \rightarrow \infty$ .

- 
- [1] M. Z. Hasan and C. L. Kane, Colloquium: Topological insulators, *Rev. Mod. Phys.* **82**, 3045 (2010).
- [2] X.-L. Qi and S.-C. Zhang, Topological insulators and superconductors, *Rev. Mod. Phys.* **83**, 1057 (2011).
- [3] D. J. Thouless, M. Kohmoto, M. P. Nightingale, and M. den Nijs, Quantized Hall conductance in a two-dimensional periodic potential, *Phys. Rev. Lett.* **49**, 405 (1982).
- [4] F. D. M. Haldane, Nonlinear field theory of large-spin Heisenberg antiferromagnets: Semiclassically quantized solitons of the one-dimensional easy-axis Néel state, *Phys. Rev. Lett.* **50**, 1153 (1983).
- [5] F. D. M. Haldane, Model for a quantum Hall effect without Landau levels: Condensed-matter realization of the ‘‘parity anomaly’’, *Phys. Rev. Lett.* **61**, 2015 (1988).
- [6] C. L. Kane and E. J. Mele, Quantum spin Hall effect in graphene, *Phys. Rev. Lett.* **95**, 226801 (2005).
- [7] K. Nomura and N. Nagaosa, Surface-quantized anomalous Hall current and the magnetoelectric effect in magnetically disordered topological insulators, *Phys. Rev. Lett.* **106**, 166802 (2011).
- [8] Y. Tanaka, T. Yokoyama, and N. Nagaosa, Manipulation of the Majorana fermion, Andreev reflection, and Josephson current on topological insulators, *Phys. Rev. Lett.* **103**, 107002 (2009).
- [9] A. Kitaev, Fault-tolerant quantum computation by anyons, *Ann. Phys. (Leipzig)* **303**, 2 (2003).
- [10] C. Nayak, S. H. Simon, A. Stern, M. Freedman, and S. Das Sarma, Non-Abelian anyons and topological quantum computation, *Rev. Mod. Phys.* **80**, 1083 (2008).
- [11] J. Alicea, Y. Oreg, G. Refael, F. von Oppen, and M. P. A. Fisher, Non-Abelian statistics and topological quantum information processing in 1D wire networks, *Nat. Phys.* **7**, 412 (2011).
- [12] R. Barends, J. Kelly, A. Megrant, A. Veitia, D. Sank, E. Jeffrey, T. White, J. Mutus, A. Fowler, B. Campbell *et al.*, Superconducting quantum circuits at the surface code threshold for fault tolerance, *Nature (London)* **508**, 500 (2014).
- [13] I. Bloch, J. Dalibard, and S. Nascimbène, Quantum simulations with ultracold quantum gases, *Nat. Phys.* **8**, 267 (2012).
- [14] M. Atala, M. Aidelsburger, J. T. Barreiro, D. Abanin, T. Kitagawa, E. Demler, and I. Bloch, Direct measurement of the Zak phase in topological Bloch bands, *Nat. Phys.* **9**, 795 (2013).
- [15] G. Jotzu, M. Messer, R. Desbuquois, M. Lebrat, T. Uehlinger, D. Greif, and T. Esslinger, Experimental realization of the topological Haldane model with ultracold fermions, *Nature (London)* **515**, 237 (2014).
- [16] M. Aidelsburger, M. Lohse, C. Schweizer, M. Atala, J. T. Barreiro, S. Nascimbène, N. R. Cooper, I. Bloch, and N. Goldman, Measuring the Chern number of Hofstadter bands with ultracold bosonic atoms, *Nat. Phys.* **11**, 162 (2015).
- [17] B. Stuhl, H. Lu, L. Aycocck, D. Genkina, and I. Spielman, Visualizing edge states with an atomic Bose gas in the quantum Hall regime, *Science* **349**, 1514 (2015).
- [18] M. Mancini, G. Pagano, G. Cappellini, L. Livi, M. Rider, J. Catani, C. Sias, P. Zoller, M. Inguscio, M. Dalmonte, and L. Fallani, Observation of chiral edge states with neutral fermions in synthetic Hall ribbons, *Science* **349**, 1510 (2015).

- [19] Z. Wu, L. Zhang, W. Sun, X.-T. Xu, B.-Z. Wang, S.-C. Ji, Y. Deng, S. Chen, X.-J. Liu, and J.-W. Pan, Realization of two-dimensional spin-orbit coupling for Bose-Einstein condensates, *Science* **354**, 83 (2016).
- [20] N. Goldman, J. Budich, and P. Zoller, Topological quantum matter with ultracold gases in optical lattices, *Nat. Phys.* **12**, 639 (2016).
- [21] H.-N. Dai, B. Yang, A. Reingruber, H. Sun, X.-F. Xu, Y.-A. Chen, Z.-S. Yuan, and J.-W. Pan, Four-body ring-exchange interactions and anyonic statistics within a minimal toric-code Hamiltonian, *Nat. Phys.* **13**, 1195 (2017).
- [22] F. D. M. Haldane and S. Raghu, Possible realization of directional optical waveguides in photonic crystals with broken time-reversal symmetry, *Phys. Rev. Lett.* **100**, 013904 (2008).
- [23] M. Hafezi, E. Demler, M. Lukin, and J. Taylor, Robust optical delay lines via topological protection, *Nat. Phys.* **7**, 907 (2011).
- [24] K. Fang, Integrated topological photonics with time-reversal symmetry breaking, in *2016 Progress in Electromagnetic Research Symposium (PIERS)* (Institute of Electrical and Electronics Engineers, Shanghai, China, 2016), pp. 803–803.
- [25] K. Fang, Z. Yu, and S. Fan, Realizing effective magnetic field for photons by controlling the phase of dynamic modulation, *Nat. Photon.* **6**, 782 (2012).
- [26] S. Sachdev, *Quantum Phase Transitions*, 2nd ed. (Cambridge University Press, Cambridge, 2011).
- [27] C.-K. Chiu, J. C. Y. Teo, A. P. Schnyder, and S. Ryu, Classification of topological quantum matter with symmetries, *Rev. Mod. Phys.* **88**, 035005 (2016).
- [28] S. Rachel, Interacting topological insulators: A review, *Rep. Prog. Phys.* **81**, 116501 (2018).
- [29] O. Dmytruk and M. Schirò, Controlling topological phases of matter with quantum light, *Commun. Phys.* **5**, 271 (2022).
- [30] T. Oka and H. Aoki, Photovoltaic Hall effect in graphene, *Phys. Rev. B* **79**, 169901(E) (2009).
- [31] N. H. Lindner, G. Refael, and V. Galitski, Floquet topological insulator in semiconductor quantum wells, *Nat. Phys.* **7**, 490 (2010).
- [32] G. L. Giorgi, S. Lorenzo, and S. Longhi, Topological protection and control of quantum Markovianity, *Photonics* **7**, 18 (2020).
- [33] B. Zhen, C. W. Hsu, Y. Igarashi, L. Lu, I. Kaminer, A. Pick, S.-L. Chua, J. Joannopoulos, and M. Soljai, Spawning rings of exceptional points out of Dirac cones, *Nature (London)* **525**, 354 (2015).
- [34] C. A. Perroni, A. De Candia, V. Cataudella, R. Fazio, and G. De Filippis, First-order transitions in spin chains coupled to quantum baths, *Phys. Rev. B* **107**, L100302 (2023).
- [35] A. Nava, C. A. Perroni, R. Egger, L. Lepori, and D. Giuliano, Dissipation-driven dynamical topological phase transitions in two-dimensional superconductors, *Phys. Rev. B* **109**, L041107 (2024).
- [36] G. De Filippis, A. de Candia, G. Di Bello, C. A. Perroni, L. M. Cangemi, A. Nocera, M. Sasseti, R. Fazio, and V. Cataudella, Signatures of dissipation driven quantum phase transition in Rabi model, *Phys. Rev. Lett.* **130**, 210404 (2023).
- [37] L. M. Cangemi, A. S. Mishchenko, N. Nagaosa, V. Cataudella, and G. De Filippis, Topological quantum transition driven by charge-phonon coupling in the Haldane Chern insulator, *Phys. Rev. Lett.* **123**, 046401 (2019).
- [38] E. J. Bergholtz, J. C. Budich, and F. K. Kunst, Exceptional topology of non-Hermitian systems, *Rev. Mod. Phys.* **93**, 015005 (2021).
- [39] Z. Gong, Y. Ashida, K. Kawabata, K. Takasan, S. Higashikawa, and M. Ueda, Topological phases of non-Hermitian systems, *Phys. Rev. X* **8**, 031079 (2018).
- [40] K. Kawabata, K. Shiozaki, M. Ueda, and M. Sato, Symmetry and topology in non-Hermitian physics, *Phys. Rev. X* **9**, 041015 (2019).
- [41] J. Hu, C. A. Perroni, G. De Filippis, S. Zhuang, L. Marrucci, and F. Cardano, Electric polarization and its quantization in one-dimensional non-Hermitian chains, *Phys. Rev. B* **107**, L121101 (2023).
- [42] A. Nava, C. A. Perroni, R. Egger, L. Lepori, and D. Giuliano, Lindblad master equation approach to the dissipative quench dynamics of planar superconductors, *Phys. Rev. B* **108**, 245129 (2023).
- [43] S. Lieu, M. McGinley, and N. R. Cooper, Tenfold way for quadratic Lindbladians, *Phys. Rev. Lett.* **124**, 040401 (2020).
- [44] D. Sénéchal, D. Perez, and M. Pioro-Ladrière, Spectral weight of the Hubbard model through cluster perturbation theory, *Phys. Rev. Lett.* **84**, 522 (2000).
- [45] David Sénéchal, D. Perez, and D. Plouffe, Cluster perturbation theory for Hubbard models, *Phys. Rev. B* **66**, 075129 (2002).
- [46] W. P. Su, J. R. Schrieffer, and A. J. Heeger, Solitons in polyacetylene, *Phys. Rev. Lett.* **42**, 1698 (1979).
- [47] W. P. Su, J. R. Schrieffer, and A. J. Heeger, Soliton excitations in polyacetylene, *Phys. Rev. B* **28**, 1138(E) (1983).
- [48] H. G. Evertz, The loop algorithm, *Adv. Phys.* **52**, 1 (2003).
- [49] Z. Wang and S.-C. Zhang, Simplified topological invariants for interacting insulators, *Phys. Rev. X* **2**, 031008 (2012).
- [50] Z. Wang and S.-C. Zhang, Strongly correlated topological superconductors and topological phase transitions via Green's function, *Phys. Rev. B* **86**, 165116 (2012).
- [51] V. Gurarie, Single-particle Green's functions and interacting topological insulators, *Phys. Rev. B* **83**, 085426 (2011).
- [52] S. R. Manmana, A. M. Essin, R. M. Noack, and V. Gurarie, Topological invariants and interacting one-dimensional fermionic systems, *Phys. Rev. B* **86**, 205119 (2012).
- [53] Z. Wang and B. Yan, Topological Hamiltonian as an exact tool for topological invariants, *J. Phys.: Condens. Matter* **25**, 155601 (2013).
- [54] In general, it is possible to define two effective Hamiltonians for the subsystem [53]: an Hermitian topological Hamiltonian, stemming from Green's function evaluated at zero frequency [useful to calculate the topological invariant through Eq. (5)], and a non-Hermitian Hamiltonian by using the poles of the Green's function, i.e., by calculating the Green's function at non vanishing frequency in the half lower complex plane. In general, the latter fails in calculating topological invariants, but it captures the quasiparticle physics. In our case, this Hamiltonian correctly reproduces also the topological invariant. The most important quantity is the renormalized energy  $\tilde{E}_k$ : at  $k = \pi$ , it becomes zero at the critical value of  $\alpha$  determining the closure and reopening of the gap.